Ground investigation of AO effect in case of complex geometry

Sophie Duzellier, David Lévêque, Claude Pons, Sabine Soonckindt
Elisabeth Laurent
Guilhem Chanteperdrix, Meggie Vilaranda-Fernandez
Pierre Jouanne, Véronique Perrin-Bailly, David Nguyen Van Sang

ONERA/DPHY, University of Toulouse, F-31055 Toulouse cedex
CNES, F-31400 Toulouse
Airbus DS, F-31400 Toulouse
Thales Alenia Space, F-06150 Cannes La Bocca

Corresponding author: Sophie Duzellier
Email: sophie.duzellier@onera.fr

ABSTRACT

Atomic Oxygen (AO) is the main component of the residual atmosphere present at low earth orbit. Multiple reflections can locally enhance or lower erosion rate in case of complex geometry. The need for precise estimate of hyperthermal AO flux is thus crucial at critical target embedded into realistic assembly.

Modeling tools (example Atomox module in ESABASE2 and SYSTEMA toolbox) may account for multiple reflections with simplistic approach (ray-tracing) and a set of semi-empirical parameters.

In this context, an original geometrical setup was designed in order to expose target surfaces with normal and tilted incidences and after one reflection on a set of materials of interest (black conductive thermal coatings, coverglass, surface treatment…). Results of two test campaigns highlights the effect of incidence angle on erosion rate (higher erosion with tilted beam) and provide an estimate of equivalent fluence after one reflection through mass loss measurement of Kapton HN foil (in the 4-10% range depending on material type).

KEYWORDS
Atomic Oxygen, scattered beam, material degradation.

DECLARATIONS

Funding: CNES R&T and co-funding of ADS and TAS
Conflict of Interest: N/A
Availability of Data and Material: N/A
Code availability: N/A

INTRODUCTION

Atomic oxygen (AO) is the main component of the residual atmosphere present at low earth orbit. The main consequence is erosion of surface materials. Some classes of materials are stable under AO attack (oxides for instance) and incoming flux is then re-emitted with specific angular and energy distributions. In case of sensitive materials, typically 90% of the incoming flux is also re-emitted. Then multiple reflections can locally enhance or lower erosion rate in case of complex geometry. The response to AO of space materials is known via measure of the erosion yield.

The issue of materials erosion by AO is mainly considered in a worth case manner i.e. with an AO flux fully directed towards exposed surface. Nevertheless in some critical applicative cases, the local geometry of sub-system may be complex (for instance: optical devices with baffles, surfaces in sight of solar panels …) where phenomena of oxygen atoms diffusion/reflection/absorption can take place, and can lead to erosion of surfaces without direct exposure to space environment.

The need for precise estimate of hyperthermal AO flux is crucial for critical target embedded into a complex geometry. Depending on the configuration, target can be partially masked or exposed to additional AO flux due to scattering. Scattering mechanisms have been reported in flight data [1, 2] and at ground studies [3].

Modeling tools (example Atomox module in ESABASE2 and SYSTEMA toolbox) may account for multiple reflections with simplistic approach (ray-tracing) and a set of semi-empirical parameters.

In this context, an original geometrical setup was designed in order to expose target surfaces with normal incidence or after one reflection. Experimental investigation was carried out to study the effect of hyperthermal AO in case of complex geometry and estimate the "secondary" AO flux after reflection on selected set of targets.

I. TEST APPROACH AND GROUND EXPERIMENTS

Ground experiment of AO multi-reflection effect can be found in the literature and address different thematic and objectives

- Investigation of local erosion enhancement linked to chamfered geometries (edge effect, [4]),
- Develop the capability to focalize AO beam at ground facility [6],
- Develop mitigation and attenuation approach to secondary thermal AO beams ([5], Figure 1),
- in 3], reflection jig was used to measure the ratio of reflected component at different angle (Figure 2).

Similarly, we designed and developed an original setup to expose target surfaces with normal incidence or after one reflection (Figure 3). Positions 1 and 2 are fitted with candidate materials whose erosion yields at normal and tilted incidence can be measured based on mass loss measurement. The configuration of the assembly also generates AO scattering on part 2 and detection of scattered flux at position 3 (reference kapton foil with known erosion yield, or active Resistack detector [7]). At position 3, it comes an estimate of the ratio of reflected AO flux received by the detector. Lastly, reference Kapton foil (position 4) is used for the measurement of the fluence level in primary (normal) beam. In practise, the Kapton erosion yield is independent of the macroscopic incident angle, using the $\cos(\theta)$ correction [6].

All MUT samples have their witness samples, i.e. samples of same geometry and same nature but that are kept safely in a dry and neutral environment, used as a reference for mass loss measurement.

Two LEOX test campaigns (AO facility at ESTEC/ESA) have been carried out each time on a set of 6 selected materials (Black Conductive Thermal Control coatings BCTC, plasma chemical coating PCC, polyimide film PI, coverglass CVG…).

II. LEOX PRELIMINARY RESULTS

Figure 4discloses the normal-to-tilted erosion yield ratio[1] for the set of materials under test (MUT). At first, it is confirmed the absence of angle influence on the erosion yield of Kapton HN considering the proposed $\cos(\theta)$ correction. For the other MUT samples, this ratio is much lower than 1 showing higher erosion yield for all tilted samples whatever the material family and type. Microscopic visual inspection is currently being carried out to compare erosion profile at normal and tilted incidence.

The values reported in Table 1 correspond to the proportion of the incident fluence after reflection on the MUT surfaces resulting in erosion of Kapton HN foils used in the detection plane. Primary-to-secondary flux ratio ranges in the 4-10% values that are of the order of magnitude of figures reported in [6] (at a different reflection angle and for different materials). Data are consistent between LEOX1 and LEOX2 even if AO incident fluence is one order of magnitude higher with LEOX2.

Visual inspection (optical) shows interesting erosion feature as disclosed in Figure 5 for PCC sample:

[1] For these estimations, the effective fluence was used (i.e. corrected by the $\cos(\theta)$ factor)

- Erosion area can be observed and measured (the white line delimits the theoretical specular zone i.e. with same incident and reflected angles),
- Clearly both specular and diffuse components add to the overall erosion of Kapton HN,
- Specular + diffuse response surface is lower than theoretical total exposed surface (not masked).

Observation of Kapton detectors for all MUT shows specific signature material-dependent. For instance, similar ratio of scattered/incident fluence were measured for PCC and CVG (resp. 8 and 10%) but the feature of visible eroded areas are very different with (see Figure 6):

- Total eroded zone is much larger for PCC,
- Eroded zone limit is convex for CVG, straight line for PCC.

The first perspective is to continue this investigation with profilometry measurements and SEM observations (currently under progress). The profilometry could help us separate specular from diffuse contribution, define with precision the additional AO erosion near the eroded perimeters …

III. ANALYSIS AND DISCUSSION (INPUTS FOR CALCULATIONS)

Besides the proof of concept of the proposed geometry, the final objective is to approximate the semi-emprirical parameters needed as input parameters for ground simulations with tools like ATOMOX (specular ratio, accommodation coefficient especially).

Obviously, many simplifying assumptions are considered in this study:

- Hard-cube model is considered here i.e. is the dominant mechanisms for AO interaction with MUT,
- The roughness of the target plane is not taken into account,
- Many reflections may take place within the assembly on lateral and top plates also.

That is why calculation with ATOMOX is planned to simulate the actual geometry and use ray tracing technic to confirm experimental observations. The main objectives are first to verify 1) the observed feature of eroded zone observed with CVG (and other MUT), i.e. convex shape limit, is due to edge effect (reflections from lateral panels), 2) the scattered fluence after a single reflection is consistent with the overall measured mass loss.

As a reminder, the calculation principle is shown in Figure 7 with main parameters:

- N Incident fluence,
- Sr/Sd specular/diffuse refleion coefficient (ex. Sr=1 fully specular, Sr=0 therefore Sd=1 fully diffuse),
- Ω Absorption coefficient (between 0 and 1),
- R accommodation ratio (between 0 and 1).

It is also assumed that $\Omega + Sr + Sd = 1$.

To help defining parameters values for all MUT, it is proposed that absorption is linked to erosion rate and accommodation to diffuse coefficient (evolve the same way). For instance, the following guideline is proposed to set the initial calculation parameters for the PCC and CVG samples:

- CVG is very resistant to AO (negligible erosion rate), a low Ω (and R parameter) shall be considered and Sr>>Sd. This “specular response” is confirmed by the “limited” eroded surface observed on the Kapton HN detector,
- PCC: erosion rate is low ($<2\ 10^{-26}$ cm^3/AO), here also a low Ω can be considered however the diffuse response is more pronounced and it is proposed to select high Sd (>Sr) and R values.

Estimate of Kapton HN parameters can be found in the literature [9, 10]. Calculations are planned in the next weeks-months. Final results and correlation, as deeper analysis (with profilometry and SEM observations), will be presented in a future paper.

IV. CONCLUSIONS

In this work, an original geometrical setup was designed in order to expose target surfaces with normal incidence or after one reflection. Candidate materials have been selected in view to compare numerical results conducted with usual modelling tools and experimental results. As already mentioned in the literature, Kapton HN was confirmed as a reference material to evaluate the level of fluence during the test campaign. Its erosion yield was confirmed to be independent of the impingement angle θ, by using the effective fluence (‘cos(θ)’ correction factor). Concerning the geometrical effect, all the materials tested with a 65°-impingement angle seem more sensitive to inclined AO erosion than normal-oriented erosion. After reflection on the inclined-MUT samples, the residual fluence coming on the detector surface is about one tenth of the direct incident fluence. The Coverglass is the more reflective material with ~10 % of transmitted fluence, other materials are between 4 and 10 %. From the optical observation of eroded Kapton films used as detectors, it’s clear the erosion area includes the area of specular reflection as well as a large diffuse reflection area, the size and the form being dependent on the reflective material.

The first perspective will be to continue the investigation on eroded surfaces by the profilometry and SEM observations. The profilometry could provide us with the border limit between specular and diffuse reflection areas and could help us to estimate a specular ratio. The SEM observations should provide a comparison of erosion states between the witness samples and the AO exposed materials in normal incidence but also with an impingement angle. Moreover some basic computations could be done to evaluate the diffuse part and the specular part of the reflected AO beam on these materials as well as the total erosion area.

V. ACKNOWLEDGMENTS

The authors acknowledge J.M. Desmarres and R. Petre Bordenave (CNES) for their valuable discussion and contribution to data analysis.

REFERENCES

1 - Bruce A. Banks et al, Lessons Learned From Atomic Oxygen Interaction With Spacecraft Materials in Low Earth Orbit, NASA/TM—2008-215264. July 2008

2 - Roger J. Bourassa et al, LDEF Atomic Oxygen Fluence Update, N93-12771, Boeing report.

3 - Yugo Kimoto et al., Simulation of Atomic Oxygen Behavior Using the NC-DSMC Method in Combined Space Effects Test Facility, proceedings of ISMSE conf. 2015.

4 - Bruce A. Banks & Sharon K. Miller, Effects of Sample Holder Edge Geometry on Atomic Oxygen Erosion Yield of Pyrolytic Graphite Exposed in Low Earth Orbit, NASA/TM—2018-219910, May 2018.

5 - Bruce A. Banks et al. Attenuation of Scattered Thermal Energy Atomic Oxygen, NASA/TM—2011-217028, April 2011.

6 - K. Yokota, M. Tagawa, and N. Ohmae, "Impingement Angle Dependence of Erosion Rate of Polyimide in Atomic Oxygen Exposures", Journal of Spacecraft and Rockets, Vol. 39, N°. 1: Engineering Notes, pp 155-156, 2002

7 - S. Duzellier et al, Validation of Atomic Oxygen Active Detector Resistack, proceedings of ISMSE conf. 2018.

8 - T. K. Minton, "Protocol for Atomic Oxygen Testing of Materials in Ground-Based Facilities", Version Number 2, JPL Publication 95-17, September 15, 1995.

9- Bruce A. Banks et al. Monte Carlo Modeling of Atomic Oxygen Interaction with Protected polymers for Projection of Materials Durability in Low Earth Orbit, Mat. Res. Soc. Vol.278, 1992.

10 – L. Chan, CH. Lee, Interaction Potential Between Atomic Oxygen and Polymer Surfaces in Low Earth Orbit, Journal of Spacecraft and Rockets, Vol.43, n°3, 2006.

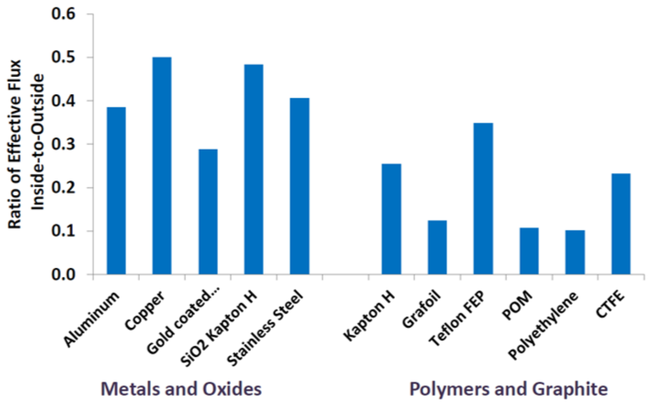

Figure 1 – ratio of effective flux detected at the bottom of an AO scattering chamber after reflection on different material species. Nasa data [5].

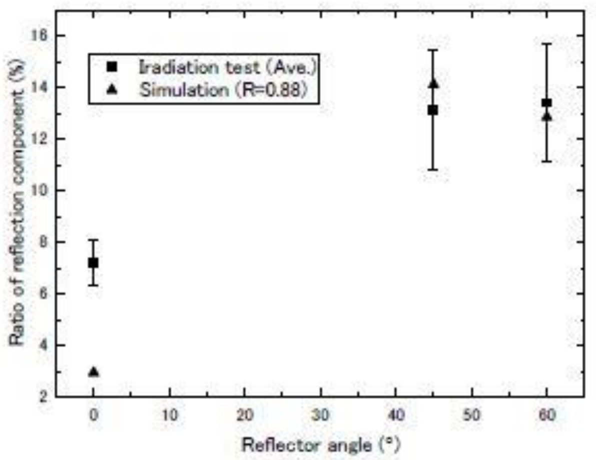

Figure 2 – Ratio of the target and number of AO particles that collided with the reference [3]

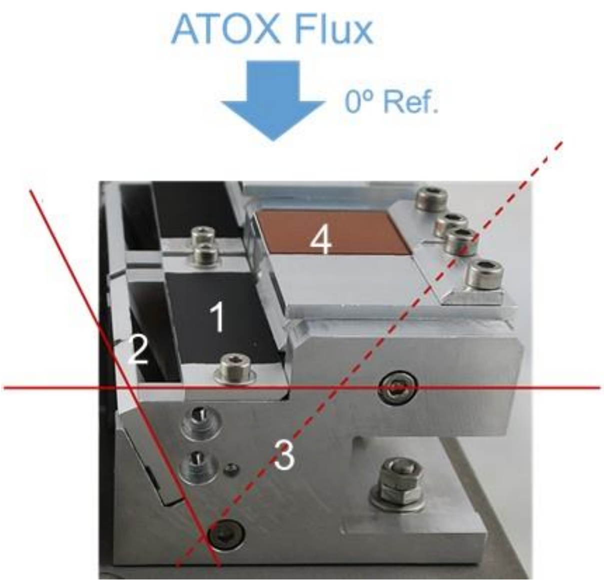

Figure 3 – experimental assembly with the different positions

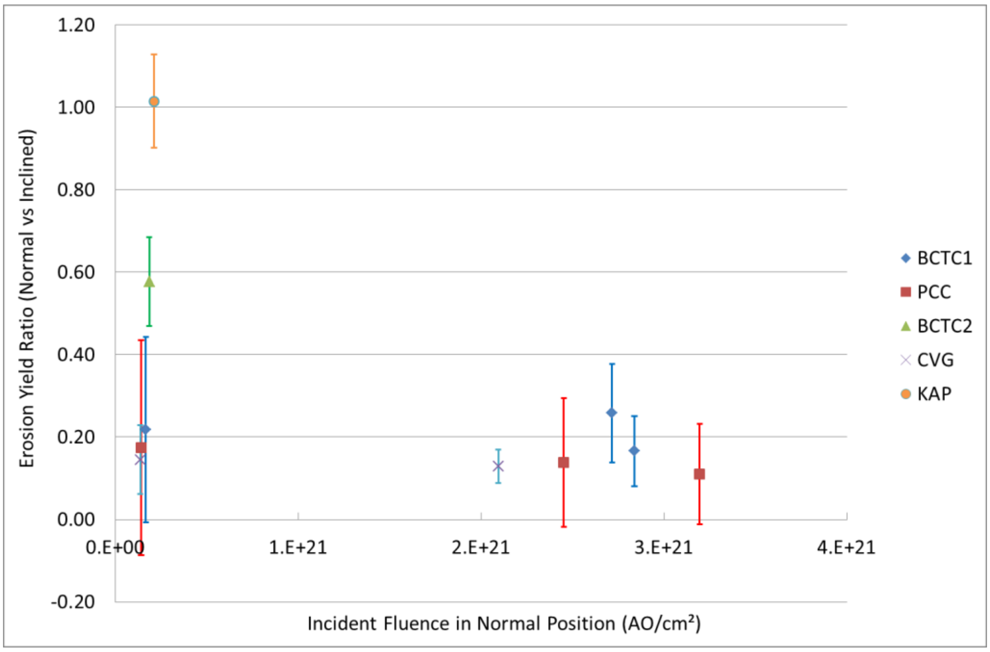

Figure 4 – Influence of impact angle (normal vs 25°) on erosion yield ratio with mean fluence LEOX1 ~1.7 10^{20} AO/cm², LEOX2 ~2.4 10^{21} AO/cm².

Table 1 – ratio in % of scattered /incident fluence for each sample type (scattered angle is 65°C) based on mass loss measurement of Kapton HN detector

Material at position 2	Ratio scattered / incident fluence	
	LEOX1 ~1.7 10^{20} AO/cm²	LEOX2 ~2.4 10^{21} AO/cm²
BCTC1	4	5
BCTC2	7	-
CVG	9	10
Kapton HN	6	-
PCC	7	8
BCTC3	-	10
Alu	7	-

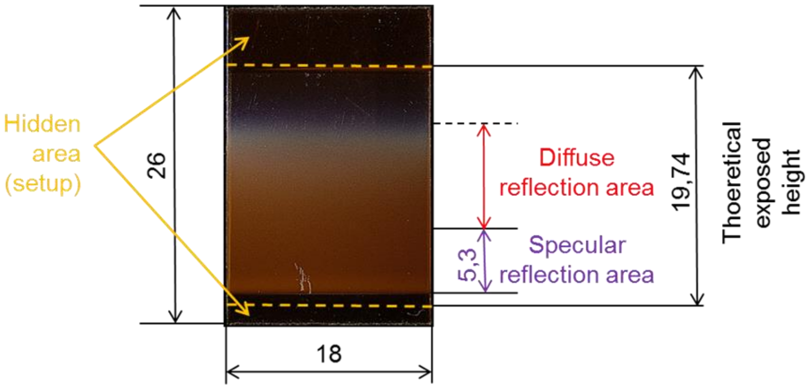

Figure 5 – picture of Kapton HN detector exposed to PCC scattered beam showing theoretical areas exposed to specular/diffuse scattered beam or masked (by parts of the assembly)

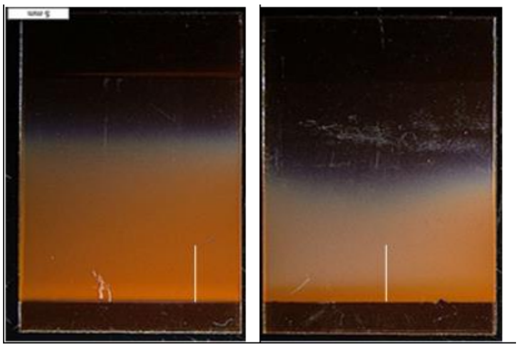

Figure 6 – pictures of Kapton HN detectors exposed to PCC (left) and CVG (right) scattered beam (the white bar indicates the limit of the specular area).

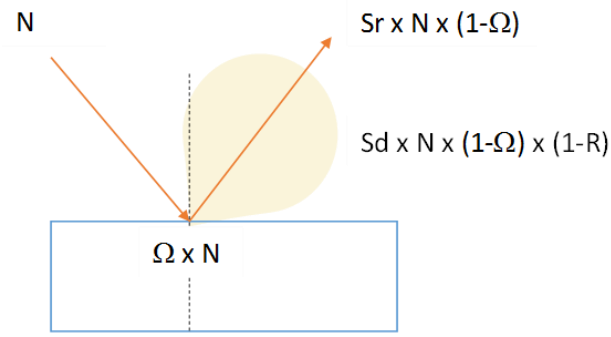

Figure 7 – ATOMOX tool: principle for calculations (ray tracing approach)